毎月ひとつの病気を取り上げ、学校・保護者・医療機関の連携や子どものQOL向上への要点などについて専門医師が解説します。

糖尿病の子どもと学校教育

雨宮　伸

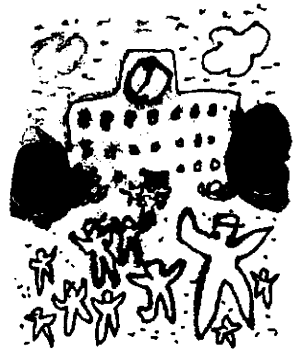

子どもの糖尿病とは

(1)成因

糖尿病は、成因によって大きくは「1型」「2型」「その他の特定の機序、疾患によるもの」に分類されます。子どもでもこの分類があてはまりますが、従来、子どもの糖尿病というと1型と考えられていました。1型糖尿病は、発症年齢が幼児期からのことも珍しくなく、生活習慣やいわゆる遺伝疾患とは直接には関係ありません。膵臓のβ細胞を自分で破壊してしまう自己免疫機序が主な原因です（機序：しくみ、操作＝編集部注）。膵臓からのインスリン分泌が枯渇していく病態が基本となりますので、インスリンの注射によってこれを補います。

注射は、各食事やおやつからの栄養を体に取り込むための食事時の「追加インスリン」といわれるものと、食事の間や夜間に脳や神経・血球などへ一定のブドウ糖（血糖）を供給するため肝臓からのブドウ糖の産生にブレーキ役となる「持続インスリン」が基本となります。つまり、一日数回の注射により血糖コントロールは維持され、このような強化インスリン療法の進歩により合併症の進展抑制は急速に改善されてきています。

2型糖尿病は従来、成人糖尿病と思われていましたが、日本では三十年前ほどから思春期以降での発症増加が認められ、肥満との関連が指摘されています。その発症の要因は、インスリン抵抗性（インスリンの効果が出にくくなること）の増大と、それを代償する（補う）ためのインスリン分泌の増加が破綻をきたすことにあります。

(2)発症リスク

人種的にも発症のリスクは異なります。欧米白人は1型糖尿病の発症リスクは日本人の二〇～三〇倍と高いのですが、2型糖尿病は近年肥満の増大が社会現象となって小児・思春期でも発症が増加しています。一方、日本人やアジア人はそれほど肥満が強くなくても、思春期での2型糖尿病が見られます。つまり、日本人ではインスリンの分泌能力が人種的に少ないので、小太り程度の肥満でもリスクとなっているのです。思春期糖尿病の二～三割は非肥満であることに注意が必要です。

また、インスリン抵抗性の増大は、肥満ばかりではありません。思春期は成長するための成長ホルモンの分泌が増えますが、このホルモンはインスリン抵抗性を生理的に作ることになるので、2型糖尿病はほとんど思春期以降に発症します。日本人では思春期の糖尿病は1型より2型糖尿病のほうが発症率は高いといわれています。

思春期2型糖尿病は、その両親および祖父母の半数以上に糖尿病の家族歴があります。しかし、特定の遺伝子が成因であることは稀で、生活習慣を含めた環境因子も発症リスクに関連する、多因子疾患です。最近は、出生時体重が二五〇〇グラム未満の子どもが年々増加しています。この低出生体重児は将来、2型糖尿病も含めた生活習慣病

＊「教育と医学」2010年6月号「特集2・慢性疾患をもつ子どもと学校教育」で現状や問題点を解説しています。併せてご活用ください（http://www.keio-up.co.jp/np/inner/30684/）。

になりやすいことも判ってきており、子宮内の胎児環境と出生後の環境の相違が、生活習慣病に関連する遺伝子に後天的に変化を与えているとも考えられています。

このように2型糖尿病の発症には、肥満をはじめとするインスリン抵抗性の増大がありますので、肥満の解消にむけた食事・運動療法が指導の基本になります。2型糖尿病となると、心・血管病変進展のリスクが高まりますので、肥満がなくても食事・運動療法は重要です。

一方、日本人は肥満であっても基本的にインスリン分泌の代償機能は少ないので、血糖コントロールに薬物療法が必要となることも多いのです。現実に思春期発症2型糖尿病の予後は1型糖尿病に比べ良くないことが知られ、網膜症、腎症など糖尿病性慢性合併症が三十歳などの若年成人で既に顕在化し、社会・経済生活に支障をきたしてしまっている場合も少なくありません。

つまり、自覚症状のないことの多い2型糖尿病では、徒に食事・運動療法に拘泥することなく、血糖コントロールが不十分であれば積極的な薬物療法の導入も必要となります。

学校生活における問題点とその対応

(1)1型糖尿病の場合

1型糖尿病においては、インスリン注射が最も子どもたちを悩ます問題です。ひんぱんな回数によるインスリン注射による強化療法が将来の合併症予防に明らかに効果があることが判っていますので、学校での受け入れ体制の不備によるインスリン注射の回避は望ましくありません。インスリン注射量の設定は、最近「カーボカウント」により決めることが多くなっています。食事内容における糖質（カーボ）量に応じたインスリン量の比によって、各食事での超速効型インスリンの注射量が決まります。したがって、給食の内容はカロリーのみならず、糖質量も予め家庭に知らされていることが必要になります。

年少児ではインスリン注射が自分でできないこともありますし、注射量の決定も難しいこともあります。そこで、昼間に注射をしない方法を選ぶことも、家族や本人の希望なら仕方ありません。インスリン注射回数や製剤の選択の権利は、本人と保護者にあります。裏返せば、将来を見すえた治療法の的確な選択へ導いてあげられるかは、医療側の科学的根拠に基づいた情報の提供と、学校での積極的対応にかかっています。

最近は超速効型インスリンのみを使って、ポンプを携帯してもらう「持続皮下インスリン注入療法（CSII）」が年少者にも導入されることがあります。食事・間食での頻回注射はかなり負担ですので、三日に一回程度皮下にカニューレ（管）を刺し入れます。食事追加インスリンも基礎インスリンもすべて、ポンプを操作してこのカニューレから投与されますので、一日数回の自己注射の必要はなくなります。いろいろな投与法をプログラムすることができますので、昼食時インスリンへの対応を家庭で設定しておくこともあります。当然、ポンプの携帯による不便も予測されますが、子どのたちの対応と受け入れは頻回注射（一日に何度か注射をする）に優るものがあります。

以上のように、学校でのインスリン注射は必須と考えるべきであり、注射をする場所の選択がしばしば問題となります。本人の了解が得られれば、教室内やどこでも注射に問題はありません。ある程度の遮蔽は必要かもしれませんが、トイレに入って注射をする子どもが多いのは改善すべき課題の一つです。また、保健室にわざわざ出向くことも少なくありませんが、その必要性は少ないと思われます。インスリン注射さえできれば、1型糖尿病の子どもに何ら学校生活への制限はありません。友達に理解を得られる状況を学校が提供できるか否かは、本人のQOL向上の基本となると考えられます。

(2)2型糖尿病の場合

2型糖尿病への学校における問題は、家庭・社会における背景も考慮する必要があり、複雑です。特に肥満を伴う子どもたちは、糖尿病の診断の前に、身体・精神的な問題を抱えていることも少なくありません。つまり、生活習慣病となる本人の成育歴の上に糖尿病が診断され、また多くの場合、明確な自覚症状を欠いていることが多いの

です。特に、学校健診における尿糖スクリーニングにおいては、糖尿病診断までとその後の療養の手引きに対する事後処置が大変曖昧なままとなっています。糖尿病のレッテルを貼られ、さらに肥満であるのは本人の生活習慣、家族の教育が悪いとしかとらえられていない場合が少なくありません。不登校・引きこもり、いじめ、片親、低収入家庭、糖尿病の家族歴など、糖尿病診断前にすでにこういった問題を抱えていることは稀でありません。

また、2型糖尿病は自覚症状が少ないため、医療機関への継続的受診が中断してしまうことも少なくありません。特に肥満2型糖尿病の診断当初は、食事および運動の療養指導のみでも血糖コントロールは一見正常化することも少なくありません。しかし、年余にわたって安定することは少なく、寛解（完全治癒ではないが、症状が軽減または消失すること）したと錯覚したり、その後の治療にむしろ難渋することもあります。継続的な受診と、解決すべき問題点と目標を明確にしてあげる必要があります。継続受診には、本人および家族への治療意欲への励ましが必須です。

学校と医療機関の連携

(1)1型糖尿病の場合

1型糖尿病における学校との連携で最も気になるのが、低血糖への対処です。低血糖となると本人自身で自分がどんな状況か判断できなくなったり、時には痙攣または意識喪失に至ることもあります。しかし、重症に見えてもほとんどの場合、回復させることができます。つまり、ブドウ糖、ペットシュガーなどの携帯または保管場所を決めておけば、無理やり口に押し込めば自然に飲みこみます。また、交感神経が亢進（高ぶり進む）し、糖新生（血中の糖が少なくなったとき、筋肉を分解し肝臓でグリコーゲン以外のものからグルコースを合成しエネルギーを作り出す現象）も回復してきます。ジュースなどは投与しやすいですが、血糖回復には時間がかかります。当然、重症なら近くの学校医やかかりつけ医でブドウ糖の注射やグルカゴン注射をできる体制を話し合っておくこともよいでしょう。

一方、低血糖は多くが自覚できます。体のだるさ、ふるえ、イラつき、冷や汗、動悸、目のかすみ、空腹感、注意力低下、顔面蒼白などです。本人が低血糖と感じたら、自分でブドウ糖、ペットシュガーなどを摂取できる環境を教師や友達に作っておいてもらえることが必要です。登下校、とくに昼の給食がない日やクラブ活動後など低血糖になりやすい場合を考え、友達に低血糖の症状を知っておいてもらうと安心です。

さらに、遠足など運動が長時間になるときは低血糖になりやすいので、予め投与するインスリン量を減らしておく必要があります。また、低血糖を防ぐため糖質を主としたおにぎりやクッキーなどを繰り返し摂取する必要があることも周知しておいてほしいことです。

また、年少者や糖尿病になって間もない時期は低血糖かどうかわからないこともあります。1型糖尿病では血糖を自分で測ることができます。この血糖自己測定を学校でもできるようにしておけば、療養体制はさらに充実するとも考えられます。

(2)2型糖尿病の場合

2型糖尿病については、継続受診と治療の遵守が予後改善の軸となります。社会・学校・家庭での課題をもつことが少なくないので、生活習慣が是正できないことを徒に非難することは、かえって療養継続の意欲をなくさせてしまいます。継続受診ができているか、学校でも食事療法・服薬が遵守できているか、励ますことの環境整備が必須です。また、肥満者では体重管理（日々の体重測定の励行）は生活習慣の改善の重要なカギになっています。一方、2型糖尿病でもインスリン注射が必要なことはあります。この場合、1型糖尿病に準じた連携も必要です。

2型糖尿病の発症リスクのひとつに、母体の痩せと妊娠中の至適体重増加の不良が問題となっています。これは、学校保健教育における課題です。ここ数年の学校保健統計では肥満児の増加抑制または軽度減少が認められてきていますが、肥満のみにとらわれず、小児メタボリックシンドロームをきちんと日本的意義を見据えて再検討すべきと考えています。

保護者との連携

(1) 1型糖尿病の場合

1型糖尿病での発症時の不安は、本人および保護者にとって大変衝撃となります。学校生活を無事過ごせるかの心配をいかに受け止めてあげるかで、その後の療養の充実に大きな違いが出ます。将来を見据えた自己管理の習熟を見守る体制について、本人、保護者、学校および医療関係者間で話し合えれば、現在のインスリン治療は学校生活や社会生活に応じた対応を可能としています。インスリンを注射するから何を食べてはいけない、低血糖が起こるかもしれないから何ができない、ということはありません。インスリンさえ適切に投与できれば、他に何も制限は必要ありません。

年少時に発症した1型糖尿病における問題のひとつに、自立の遅れがあります。インスリン投与量の設定や注射に保護者の介助を必要としていた子どもにとって、昼食への対応や補食についての自立には学校側との連携は不可欠です。いつまでも保育園、幼稚園、学校へ家族が出向くのは、子どもの自立にとっても不自然ですし、友人関係の促進に妨げとなります。

1型糖尿病においては、糖尿病キャンプが全国的に各地で開催されており、年少者への自立支援、自己血糖測定、自己注射、さらに1型糖尿病の仲間作りが企画されています。1型糖尿病の年少者もこのような環境の中にいると、自立はそんなに難しいことではないことが観察されます。学校関係者も過度に防衛的にならず、また家族も過度に保護的または学校への過度の期待を前提としないでも、子どもたちは常に自立の用意があると考えられます。

(2) 2型糖尿病の場合

2型糖尿病ではやはり、本人および家族全体への支援体制を、学校のみならず社会の問題として考える必要があります。小児慢性特定疾患支援事業のなかに糖尿病は含まれますが、2型糖尿病については薬物療法を受けていることが前提になり、支援の体制が不十分になりがちなことは否め

「糖尿病患児の治療・緊急連絡法等の連絡表」　（日本学校保健会の提供による）

糖尿病患児の治療・緊急連絡法等の連絡表

学校名　　年　組　　記載日 平成　年　月　日
医療機関
氏名　　男・女　　医師名　　印
生年月日 昭和・平成　年　月　日　　電話番号

要管理者の現在の治療内容・緊急連絡法

診断名　①1型（インスリン依存型）糖尿病　②2型（インスリン非依存型）糖尿病
現在の治療　1. インスリン注射：　1日　回　　昼食前の学校での注射（有・無）
学校での自己血糖値測定（有・無）
2. 経口血糖降下薬：薬品名（　　）学校での服用（有・無）
3. 食事・運動療法のみ
4. 受診回数　　回／月
緊急連絡先　保護者　氏名　　自宅TEL
勤務先（会社名　　TEL　　）
主治医　氏名　　施設名　　TEL

学校生活一般：基本的には健常児と同じ学校生活が可能である

1. 食事に関する注意
学校給食　①制限なし　②お代わりなし　③その他（　　）
宿泊学習の食事　①制限なし　②お代わりなし　③その他（　　）
補食　①定時に（　時　食品名　　）
②必要なときのみ（どういう時　　）
（食品名　　）
③必要なし
2. 日常の体育活動・運動部活動について
「日本学校保健会　学校生活管理指導表」を参照のこと
3. 学校行事（宿泊学習、修学旅行など）への参加及びその身体活動
「日本学校保健会　学校生活管理指導表」を参照のこと
4. その他の注意事項

低血糖が起こったときの対応*

程度	症状	対応
軽度	空腹感、いらいら、手がふるえる	グルコース錠2個（40kcal=0.5単位分。入手できなければ、スティックシュガー10g）
中程度	黙り込む、冷汗・蒼白、異常行動	グルコース錠2個（あるいは、スティックシュガー10g） さらに多糖類を40~80kcal（0.5~1単位分）食べる。 （ビスケットやクッキーなら2~3枚、食パンなら1/2枚、小さいおにぎり1つなど） 上記補助食を食べた後、保健室で休養させ経過観察する。
高度	意識障害、けいれんなど	保護者・主治医に緊急連絡し、救急車にて主治医または近くの病院に転送する。救急車を待つ間、砂糖などを口内の類粘膜になすりつける。

＊軽度であっても低血糖が起こったときは、保護者・主事医に連絡することが望ましい。

ません。生活習慣の是正が必要な場合、その家族内では解決できない問題も少なくありません。2型糖尿病については、キャンプのような療養指導の場も少なく、経済的負担からキャンプのような場が企画されても参加は容易ではありません。また、単なる肥満防止キャンペーンでは、現実の2型糖尿病の子どもへの支援としては不十分です。小児科医、内科医、糖尿病・内分泌専門医が今後さらに真剣に取り組むべき時期にきているようです。

子どものQOL向上のため

糖尿病の子どもたちおよび保護者のQOLを同年齢の非糖尿病の子どもと比較した研究がなされています。詳細は報告書を参考にしてください。日本でのその報告の内容から筆者が感じていることを若干述べます。

1型糖尿病の子どもたちのQOLは、子どもも保護者も総じて悪くないとされています。前述してきたように、1型糖尿病の少ない日本では、欧米に比べ社会・学校での理解が乏しいぶん、保護者が懸命に支援体制を連携して構築していると思われます。また、全国各地での糖尿病サマーキャンプも日本糖尿病協会が中心となって行われるようになり、財政的支援もある程度あります。キャンプの運営も医療関係者から保護者主体になりつつあり、キャンプ参加の経験のある青年たちがキャンプの運営に協力している姿が多くなりました。

しかし、欧米のように1型糖尿病の子どもが周囲に多くいる社会でのQOLに比して、日本では決して満足がいくものとしては報告されていません。ここには、血糖コントロールを改善する様々な特徴を持つインスリン製剤の開発やポンプや人工膵臓などの治療技術の向上のみでは解決できない患者および保護者の苦悩が存在し、QOLの改善にはまだ遠いことを意味していると考えます。そして、日本におけるQOLの見かけ上の満足は、やはり子どもたちの自立に対し、我々医療者、社会、学校、保護者、本人に未熟な面が残されている裏返しかもしれないと考えています。

国際的にも、QOLの向上をめざした取り組みが国際糖尿病連合（IDF）と国際小児・思春期糖尿病学会（ISPAD）においてDAWN YOUTH（DAWN: Diabetes Attitudes, Wishes and Needs）として行われており、日本からも参加して意見交換がなされています。また、肥満の増加と小児2型糖尿病の増加は「パンデミック」として注目を浴びている世界的な課題です。共通の認識はありますが、この子どもたちのQOLの低さは、経済格差の広がりとも関連があり、容易に改善の道は拓かれないと思われます。糖尿病と貧困の再生産に陥らないよう、世代を超えてライフサイクルのどの時点でも有効な介入が期待されます。

糖尿病は、1型であれ2型糖尿病であれ、早期の血糖管理がその後十数年にわたっての合併症進展に影響することが判ってきました。このような早期血糖管理の遠隔効果をそれぞれ、「メタボリック　メモリー」および「遺産効果（legacy effect）」といいます。残された人生を糖尿病と付き合っていかねばならない小児・思春期発症糖尿病をもつ子どもたちへの支援は、本人、家族のみならず、学校・社会全体が果たす役割が大きいのです。

[参考図書]
1)日本小児内分泌学会糖尿病委員会編『こどもの1型糖尿病ガイドブック――患児とその家族のために』文光堂、二〇〇七年
2)日本糖尿病学会（編）『小児・思春期糖尿病管理の手びき』南江堂、二〇〇七年
3)雨宮伸「新時代の糖尿病学(3)：小児糖尿病患者・家族への教育」、『日本臨床』66：suppl7, pp497-501, 二〇〇八年

●雨宮　伸（あめみや・しん）
埼玉医科大学小児科教授。医学博士。専門は小児内分泌・糖尿病。慶應義塾大学医学部卒業。慶應義塾大学医学部、イリノイ大学医学部、地域基幹病院等、山梨大学医学部小児科助教授を経て現職。著書に『小児・思春期糖尿病管理の手びき〈改訂第2版〉』（編集責任者、南江堂、二〇〇七年）、『こどもの1型糖尿病ガイドブック』（編集責任者、文光堂、二〇〇七年）など。

＊次回は「てんかんの子どもと学校教育」です。

Human Molecular Genetics, 2011, Vol. 20, No. 7 **1274–1284**
doi:10.1093/hmg/ddq568
Advance Access published on January 3, 2011

Wolfram syndrome 1 gene (*WFS1*) product localizes to secretory granules and determines granule acidification in pancreatic β-cells

Masayuki Hatanaka[1,2], Katsuya Tanabe[1], Akie Yanai[3], Yasuharu Ohta[1], Manabu Kondo[1], Masaru Akiyama[1], Koh Shinoda[3], Yoshitomo Oka[4] and Yukio Tanizawa[1,*]

[1]Division of Endocrinology, Metabolism, Hematological Sciences and Therapeutics, Department of Bio-Signal Analysis, [2]Department of Diabetes Research and [3]Division of Neuroanatomy, Department of Neuroscience, Yamaguchi University Graduate School of Medicine, Ube, Yamaguchi, Japan and [4]Division of Molecular Metabolism and Diabetes, Tohoku University Graduate School of Medicine, Sendai, Miyagi, Japan

Received October 15, 2010; Revised and Accepted December 29, 2010

Wolfram syndrome is an autosomal recessive disorder characterized by juvenile-onset insulin-dependent diabetes mellitus and optic atrophy. The gene responsible for the syndrome (*WFS1*) encodes an endoplasmic reticulum (ER) resident transmembrane protein. The *Wfs1*-null mouse exhibits progressive insulin deficiency causing diabetes. Previous work suggested that the function of the WFS1 protein is connected to unfolded protein response and to intracellular Ca^{2+} homeostasis. However, its precise molecular function in pancreatic β-cells remains elusive. In our present study, immunofluorescent and electron-microscopic analyses revealed that WFS1 localizes not only to ER but also to secretory granules in pancreatic β-cells. Intragranular acidification was assessed by measuring intracellular fluorescence intensity raised by the acidotrophic agent, 3-[2,4-dinitroanilino]-3′-amino-*N*-methyldipropyramine. Compared with wild-type β-cells, there was a 32% reduction in the intensity in WFS1-deficient β-cells, indicating the impairment of granular acidification. This phenotype may, at least partly, account for the evidence that *Wfs1*-null islets have impaired proinsulin processing, resulting in an increased circulating proinsulin level. Morphometric analysis using electron microscopy evidenced that the density of secretory granules attached to the plasma membrane was significantly reduced in *Wfs1*-null β-cells relative to that in wild-type β-cells. This may be relevant to the recent finding that granular acidification is required for the priming of secretory granules preceding exocytosis and may partly explain the fact that glucose-induced insulin secretion is profoundly impaired in young prediabetic *Wfs1*-null mice. These results thus provide new insights into the molecular mechanisms of β-cell dysfunction in patients with Wolfram syndrome.

INTRODUCTION

Diabetes mellitus is a heterogeneous disorder characterized by glucose intolerance that affects over 170 million people worldwide (1). The disease arises from a combination of absolute (type 1) or relative (type 2) insulin deficiency with variable peripheral insulin resistance. The failure of insulin supply is implicated to result from both impaired β-cell function and decreased β-cell mass (2–4).

Wolfram syndrome (OMIM 222300) is an autosomal recessive disorder with severe neurodegeneration. Affected individuals present with juvenile-onset insulin-dependent diabetes mellitus and optic atrophy (5). Postmortem studies of the pancreas from patients with Wolfram syndrome have revealed a selective β-cell loss (6). The gene responsible for the disorder, *WFS1*, encodes a novel transmembrane protein (7,8). The WFS1 protein, also called Wolframin, consists of 890 amino acids and is predicted to have nine membrane-spanning

*To whom correspondence should be addressed at: Division of Endocrinology, Metabolism, Hematological Sciences and Therapeutics, Yamaguchi University Graduate School of Medicine, 1-1-1 Minamikogushi, Ube, Yamaguchi 755-8505, Japan. Tel: +81 836222250; Fax: +81 836222342; Email: tanizawa@yamaguchi-u.ac.jp

domains. This protein is known to be embedded in the endoplasmic reticulum (ER) membrane (9). Mice with a disrupted *Wfs1* gene exhibit a selective β-cell loss. This phenotype has been thought to result from the activation of ER stress, impaired cell cycle progression and apoptosis (10–14). In addition, insulin secretion from the isolated islets of *Wfs1*-null mice was shown to be impaired (15). An early study has shown that WFS1 might serve directly as a divalent ion channel or, alternatively, as a regulator of existing channel activity (16). Later, it was demonstrated that WFS1 positively modulates the Ca^{2+} level in ER by increasing the rate of Ca^{2+} uptake (10). However, the lack of distinct domains in WFS1 makes it difficult to understand its precise physiological function in pancreatic β-cells.

Secretory granules are acidified through a proton gradient, established and maintained by coordinated action between H^+-pumping vacuolar-type ATPase (V-ATPase) (17) and ClC-3, a chloride ion channel (18). The low pH of late secretory granules is necessary for proinsulin processing, and in addition, for the priming of the granules preceding exocytosis (18).

In this study, WFS1 was found to localize not only in ER but also in dense-core secretory granules in pancreatic β-cells. *Wfs1*-null mice exhibited severely impaired insulin secretion in response to glucose. These observations prompted us to investigate the functional significance of the granule-resident WFS1 protein, including its role in the acidification of insulin secretory granules, as an additional physiological function of WFS1.

RESULTS

WFS1 protein localizes to insulin secretory granules

Previous studies have shown that the majority of WFS1-immunoreactive cells were insulin-producing β-cells (16,19) in pancreatic islets. However, the precise intracellular localization of WFS1 in β-cells has not been examined, whereas this protein is thought to localize predominantly in ER in WFS1-overexpressing heterologous cells (7,9,11,20). We thus attempted to detail its intracellular localization to obtain a clue to understand further physiological roles of WFS1 in pancreatic β-cells. Immunohistochemical analysis of pancreatic sections from wild-type (*Wt*) animals using anti-WFS1 antibodies and antibodies against markers for either ER or secretory granules was performed. As shown in Figure 1A–C, only a little part of the immunoreactive area for WFS1 protein (red) appeared to merge with that for Grp78, an ER marker (green). Surprisingly, there appeared to be better co-localization of WFS1 protein with chromogranin A (green), a marker of secretory granules (Fig. 1D–F). To further substantiate the localization of WFS1 protein to the secretory granule, immunoelectron microscopy using anti-WFS1 antibodies was performed. β-Cells could be distinguished from α- and δ-cells by the appearance of the secretory granules. β-Cell granules have a white halo, which is not apparent in α- and δ-granules. As described previously (19), immunoreactivity for WFS1 protein was observed in β-cells but not in α-cells (Fig. 1G). As shown in Figure 1H, there appeared to be the accumulation of immunoreactivity not only in ER but also in dense-core granules in *Wt* β-cells. High magnification more clearly showed accumulation of immunoreactivity in the periphery of electron-dense-core granules accompanied by a halo in *Wt* β-cells (Fig. 1I). Consistently, no immunoreactivity for WFS1 was observed in WFS1-deficient β-cells (Fig. 1J). These results clearly demonstrate that WFS1 localizes not only in ER but also in secretory granules in pancreatic β-cells. The intracellular distribution of WFS1 in pancreatic β-cells was assessed by immunogold electron microscopic analysis (Fig. 1K–M). We quantified the labeling by counting gold particles per β-cell area and found ~40% more immunogold particles in secretory granules relative to those in ER (Fig. 1M). No particles were found in mitochondria. From these immunohistological observations at the tissue and ultrastructural levels, we concluded that WFS1 preferentially localizes in dense-core granules in pancreatic β-cells.

WFS1 deficiency impairs intragranular acidification

Of interest to the function of WFS1, despite a lack of distinct domains in WFS1, it has nine membrane-spanning domains, enabling us to expect that this protein may function as an ion-channel regulator. We hypothesized that WFS1 in insulin granules might play a role in the regulation of acidification of insulin granules. To test this hypothesis, granular acidification was examined by incubating mechanically dispersed islet cells with the acidotrophic agent 3-[2,4-dinitroanilino]-3′-amino-*N*-methyldipropyramine (DAMP) (21,22). Insulin-producing cells were selected by co-staining for insulin. Indirect immunofluorescence intensity, raised by DAMP accumulation, in the whole cell with the exception of the nucleus was measured. The number of lysosomes in β-cells is negligible compared with insulin granules (estimated as 48 and 11 000 per β-cell, respectively) (17) and, therefore, will not significantly contribute to the fluorescent signal. Indirect immunofluorescence intensity for DAMP (green) in insulin immunoreactive cells from *Wfs1*$^{-/-}$ mice appeared to be weaker than that in insulin immunoreactive cells from *Wt* mice (Fig. 2A–I). *Wfs1*$^{-/-}$ β-cells had significantly reduced immunofluorescence intensity to an average of 68% of the average intensity of *Wt* β-cells (Fig. 2J). *Wt* β-cells incubated with bafilomycin A1, a V-ATPase inhibitor, exhibited an even larger reduction in intensity. These observations were replicated when granular acidification was assessed using LysoTracker, another acidotrophic probe (Fig. 2K). Hence, these results strongly suggest that WFS1 plays a role in maintenance of acidification in dense-core granules of pancreatic β-cells.

Islets from WFS1-deficient mice have impaired insulin processing

Processing of proinsulin into mature insulin requires cleavage by the prohormone convertase enzymes, PC1/3 and PC2 (23–25). These enzymes have an acidic optimum pH (23), and the conversion of proinsulin to insulin is strictly dependent on a low pH (24,26). We thus hypothesized that proinsulin conversion to insulin might be affected by impaired intragranular acidification in WFS1-deficient β-cells. To test this hypothesis, the amounts of insulin and proinsulin in isolated islets

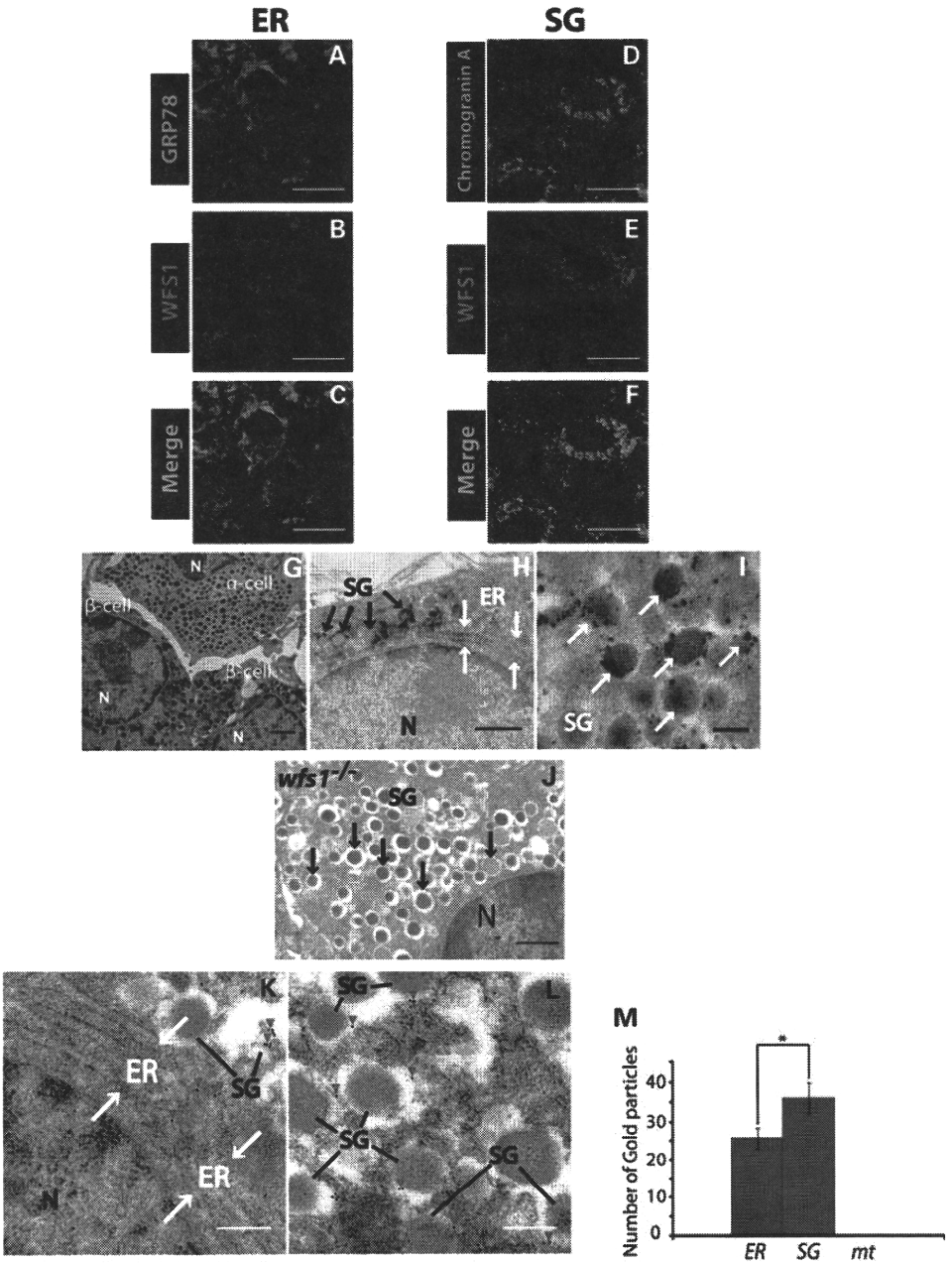

Figure 1. Localization of WFS1 to secretory granules (SG) in pancreatic β-cells. (**A**–**F**) Immunofluorescence analysis of pancreatic islets of *Wt* mice using antibodies to WFS1 (B and E, red) and antibodies to either GRP78 (A, green) or chromogranin A (D, green). Scale bars represent 10 μm. Immunoelectron microscopy of WFS1 with the DAB method, performed on pancreatic sections from $Wfs1^{-/-}$ and *Wt* mice (**G**–**J**). (G) Representative electron micrograph showing the localization of WFS1 in β-cells but not in α-cells. Scale bar represents 1 μm. Red arrow heads indicate WFS1 immunoreactivity. (H) Representative areas of β-cell from *Wt* mice. Scale bars represent 500 nm. (I) High magnification of representative dense-core secretory granules in β-cell from *Wt* mice. Scale bar represents 200 nm. (J) Representative area of β-cell from $Wfs1^{-/-}$ mice. Scale bars represent 500 nm. (**K** and **L**) Distribution of WFS1 in pancreatic β-cells. The distribution of WFS1 is shown by immunogold labeling (red arrow heads indicate examples). Bar: 200 nm. (**M**) Gold particle frequency in ER and SG per β-cell area (36 μm^2 × 24 sections). SG, secretory granule; ER, endoplasmic reticulum; mt, mitochondria.

from mice at 12 weeks of age were examined by western blot. As shown in Fig. 3A, there was a significant reduction in the abundance of mature insulin relative to GAPDH, a control for protein loading, in $Wfs1^{-/-}$ islets compared with that in *Wt* mice (Fig. 3B), whereas the proinsulin level was not altered (Fig. 3C). There was a consistent parallel increase in the proinsulin to insulin ratio in $Wfs1^{-/-}$ islets relative to that in *Wt* islets (Fig. 3D), indicating that the lack of WFS1 causes impaired insulin processing. In accordance with this observation, the plasma proinsulin level after 6 h fasting was higher in WFS1-deficient mice than in *Wt* mice (Table 1). Expression levels of prohormone convertases were further examined. As shown in Figure 3E, there was a significant reduction in the PC1/3 level in $Wfs1^{-/-}$ islets relative to

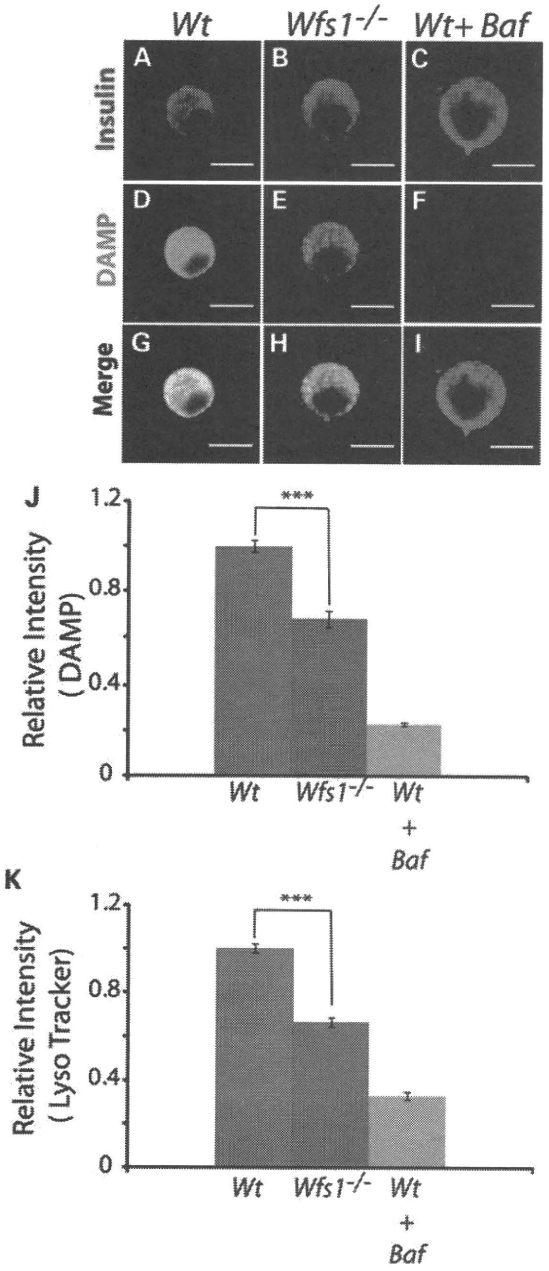

Figure 2. Disturbed intragranular acidification in WFS1-deficient β-cells. Dispersed islet cells from *Wfs1*$^{-/-}$ and *Wt* mice were incubated with either 3 μM DAMP or 25 nM LysoTracker for 1 h or 30 min, respectively, and were then fixed. (**A**–**I**) Representative photographs of DAMP-incubated islet cells stained with antibodies to DNP (green) and insulin (red). Treatment of *Wt* islet cells with bafilomycin A1 was a control of disturbed intragranular acidification. (**J**) Mean fluorescence intensity of DNP per area of each insulin-immunoreactive cell was measured. The results were obtained from 76 randomly selected *Wfs1*$^{-/-}$ β-cells and 65 *Wt* β-cells from nine different animals of each genotype. Relative intensity was expressed as the mean ± SEM. ***$P < 0.001$. (**K**) Relative mean fluorescence intensity of LysoTracker per area of each insulin-immunoreactive cell was calculated in a total of 167 *Wt* β-cells and 170 *Wfs1*$^{-/-}$ β-cells from six different animals of each genotype and graphically expressed as the mean ± SEM. ***$P < 0.001$.

that in *Wt* islets, whereas the PC2 level was not altered (Fig. 3F and G). In *Wfs1* haploinsufficiency (*Wfs1*$^{+/-}$) islets, no appreciable changes were observed in either proinsulin processing or PC1/3 expression (data not shown). To further examine the mechanism linking the lack of WFS1 to the reduced PC1/3 level, immunoprecipitation analysis using anti-WFS1 antibody was performed. However, a direct interaction of WFS1 with PC1/3 was not proved (data not shown).

WFS1 plays a role in regulation of insulin secretion *in vivo*

It has been documented that islets isolated from *Wfs1*$^{-/-}$ mice exhibited a decrease in insulin secretion in response to glucose (15). We further examined the effect of lack of WFS1 on *in vivo* insulin secretion in response to glucose at 12 weeks of age. At this age, the non-fasting blood glucose level of *Wfs1*$^{-/-}$ mice was similar to that of *Wt* mice (Fig. 4A). Glucose tolerance tests were then conducted. Blood glucose levels after overnight fasting were indistinguishable between the mutant mice and the *Wt* mice. The blood glucose level at 60 min after intraperitoneal glucose injection in WFS1-deficient mice was slightly but significantly increased relative to that in *Wt* mice (Fig. 4B). Insulin secretory response to glucose was then assessed. Whereas there was no significant change in the insulin level after overnight fasting, serum insulin levels at 2 and 15 min after glucose challenge were markedly reduced in *Wfs1*$^{-/-}$ mice compared with those in *Wt* mice. The reduced insulin levels in *Wfs1*$^{-/-}$ mice persisted until 30 min after glucose injection (Fig. 4C).

The effect of WFS1 deficiency on the β-cell mass at this age was examined. As shown in Figure 4D, insulin-positive cells still appeared to be maintained in 12-week-old WFS1-deficient mice. The insulin-immunoreactive area in WFS1-deficient mice was indistinguishable from that in *Wt* mice (Fig. 4E). Consistently, whole pancreatic insulin content was maintained in WFS1-deficient mice compared with that in *Wt* mice (Fig. 4F). These results indicate that WFS1-deficient mice have severely impaired insulin secretion in response to glucose, when abundance of β-cells is still maintained, before progressive β-cell loss becomes apparent.

WFS1 deficiency results in reduction in plasma membrane-attached secretory granules in pancreatic β-cells

To further examine the effects of WFS1 deficiency, the morphological characteristics of dense-core granules were studied by an electron microscopic analysis of pancreatic sections from randomly fed 12-week-old mice. There were no apparent differences in the appearance of electron-dense-core granules between *Wfs1*-null and *Wt* β-cells, whereas mild dilatation of ER was shown in some WFS1-deficient β-cells, as described previously (11,14) (Fig. 5A). There was no significant difference in granule size assessed by measuring granule diameter (Fig. 5B). Granule density (granule number per cytosolic area) was not affected in WFS1-deficient β-cells (Fig. 5C), either. On the other hand, the density of insulin granules docking to the plasma membrane appeared to be decreased. In fact, the number of insulin granules directly attached to the plasma membrane per cytosolic area (Fig. 5E) and per granule density (Fig. 5F) was significantly reduced in *Wfs1*$^{-/-}$ β-cells compared with that in *Wt*

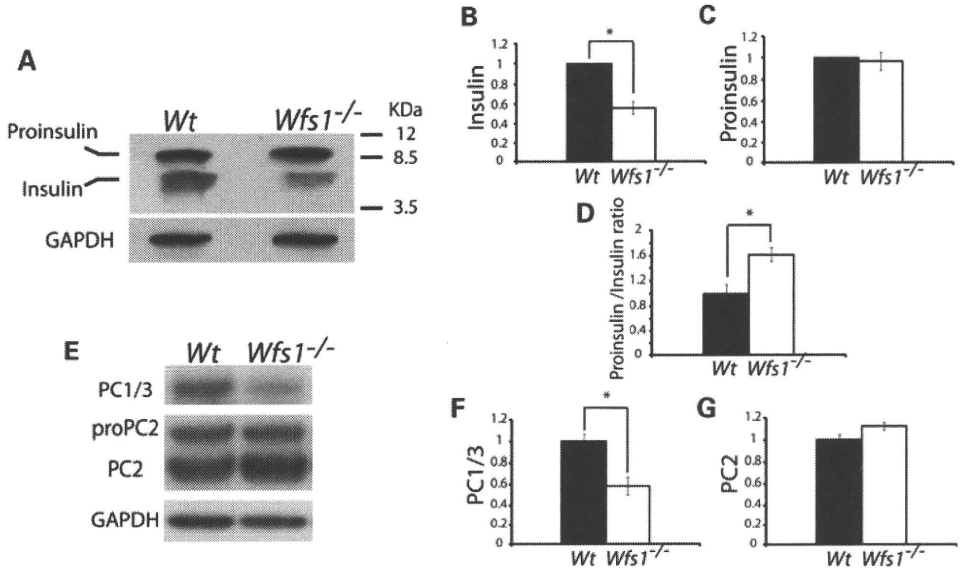

Figure 3. Impaired insulin processing in WFS1-deficient β-cells. Islets were isolated from 12-week-old *Wfs1*$^{-/-}$ and *Wt* mice. (**A**) Western blot analysis with antibodies to insulin and GAPDH. Representative results of multiple independent experiments are presented. Densities of mature insulin and proinsulin were measured and normalized to GAPDH. The results for insulin versus GAPDH (**B**), proinsulin versus GAPDH (**C**) and relative proinsulin/insulin ratio (**D**) are graphically illustrated as the mean ± SEM. $^{*}P < 0.05$. (**E**) Western blot analysis with anti-PC1, anti-PC2 and anti-GAPDH antibodies. Representative results from four independent experiments are presented. (**F** and **G**) Densities of PC1 and PC2 were measured and normalized to GAPDH. Mean protein levels ± SEM are summarized in the graph. $^{*}P < 0.05$.

β-cells. These results suggest that WFS1 function somehow determines the intracellular distribution of secretory granules, especially the docking of insulin granules to the plasma membrane. This defect may underlie, at least in part, the impairment of glucose-stimulated insulin secretion and hence may play a role in the regulation of the insulin secretory pathway.

DISCUSSION

The combination of β-cell dysfunction and β-cell loss results in progressive insulin deficiency in *Wfs1*-null mice. WFS1 has been thought to be connected with unfolded protein response and intracellular Ca^{2+} homeostasis. The present study provides additional insights into the physiological role of WFS1 in pancreatic β-cells. The following observations were documented: (i) WFS1 protein localizes in secretory granules in pancreatic β-cells; (ii) lack of WFS1 results in disturbed intragranular acidification; (iii) WFS1 deficiency causes impaired conversion of proinsulin to insulin accompanied by a decreased PC1/3 protein level; (4) WFS1-deficient β-cells have a reduced number of dense-core vesicles attached to the plasma membrane, possibly providing cellular evidence correlated with impaired insulin secretion. Taken together, these findings provide additional insights into the mechanisms of β-cell dysfunction in Wolfram syndrome.

In our present study, histological analysis at the tissue level and the ultrastructural level revealed that WFS1 was expressed not only in ER but also in dense-core granules in mouse pancreatic β-cells. In addition, immunogold particles against WFS1 were detected rather more abundantly in dense-core granules than in ER, indicating that WFS1 in dense-core granules as well as in ER could be required for sufficient β-cell function. In this regard, WFS1-deficient β-cells exhibited disturbed intragranular acidification. Because a number of membrane proteins in dense-core granules participate in important processes, such as vesicle trafficking or generation of intragranular acidification, impaired intragranular acidification is likely to result from the defect of WFS1 in dense-core granules. Intragranular acidification depends on the simultaneous operation of the V-type H^{+}-ATPase and the ClC-3 Cl^{-} channel on the insulin granule membrane (18). Although the present study did not address how WFS1 contributes to the maintenance of intragranular acidification, the function of WFS1 in insulin granules could be connected with the regulation of these channel activities.

Impaired proinsulin processing was documented in WFS1-deficient islets. Granted the impaired vesicular acidification, this is an expected and confirmatory result because acidic pH in insulin granules is required for sufficient endopeptidase activities of PC1/3 and PC2, and hence efficient proinsulin processing (23). In addition, we observed that the PC1/3 level but not the PC2 level was decreased in WFS1-deficient islets. The reduced PC1/3 level may contribute to a further reduction in endopeptidase activity of PC1/3. However, a direct link between lack of WFS1 and reduced PC1/3 level has not been proved. Exact mechanisms by which WFS1 deficiency causes reduced PC1/3 levels are unclear at this stage. Both PC1/3 and PC2 are expressed in the β-cells, whereas only PC2 is predominantly expressed in α-cells (27). If β-cells were selectively lost, decrease in PC1/3 protein would be apparent compared with PC2 in total islets. However, this is not the case because β-cell mass is not decreased at this age (Fig. 4D–F).

Secretory granules in β-cells can be divided into the readily releasable pool (RRP) and the reserve pool (28–30). The process in which granules proceed from the reserve pool

Table 1. Serum insulin and proinsulin level of 12–16-week-old mice after a 6 h fast

Genotype	Blood glucose (mg/dl)	Serum insulin (ng/ml)	Serum proinsulin (ng/ml)	Proinsulin/insulin (%)	Number
Wt	185 (±9)	0.34 (±0.03)	0.026 (±0.005)	4.6 (±0.8)	9
Wfs1$^{-/-}$	182 (±11)	0.47 (±0.05)	0.050 (±0.006)*	7.0 (±1.0)	9

*$P < 0.01$ by one-factor Student's *t*-test compared with *wt* mice.

into the RRP is referred to as mobilization and involves priming by ATP hydrolysis. A recent study demonstrated that acidification of the secretory granules is necessary for the priming of the granules preceding excytosis (18,22,31,32). We observed that the number of dense-core granules attached to the plasma membrane was reduced in β-cells of *Wfs1*-null mice, in association with impaired granular acidification. Docking and priming precede the Ca^{2+}-evoked exocytic granular fusion events, and thus this observation may explain, at least in part, the impaired glucose-stimulated insulin secretion, another pathologic feature of β-cells, in *Wfs1*-null mice.

What is the molecular function of WFS1 protein? Current information on this fundamental question is very limited. As mentioned earlier, WFS1 protein may be a channel/transporter or its functional regulator (10,16). Calcium, protons or chloride channels are candidates in ER and in the insulin secretory granules for regulation of ER calcium homeostasis or secretory granule acidification. It was also reported that WFS1 protein bound to the sodium–potassium ATPase b1 subunit (33) and calmodulin (34), although the functional significance of binding to these target molecules is unknown. Very recently, WFS1 was reported to negatively regulate activating transcription factor 6α through the ubiquitin–proteasome pathway (35). According to this finding, WFS1 may regulate target protein function, by modulating their turnover. Clearly, WFS1 can regulate multiple cellular functions and play a different role in each compartment in pancreatic β-cells.

In conclusion, previous studies have shown that WFS1 is an ER transmembrane protein that is implicated in cellular Ca^{2+} homeostasis and unfolded protein response in β-cells. Our present study has demonstrated that the WFS1 protein is also localized to the secretory granules in mouse pancreatic β-cells and suggested its functional significance. The current study provides new insights into WFS1 protein function and the pathophysiology of Wolfram syndrome.

MATERIALS AND METHODS

Animal production and metabolic phenotype analysis

Generation and genotyping of *Wfs1*$^{-/-}$ mice have been described previously (15). We maintained *Wfs1*$^{-/-}$ mice on a C57BL/6J background. For the glucose tolerance test, mice were subjected to overnight fasting followed by intraperitoneal glucose injection (2.0 g/kg). Blood glucose was measured at 0, 15, 30 and 60 min after injection using an automatic blood glucose meter, Antsense III (Horiba, Kyoto Japan). Blood samples were collected at 0, 2, 5, 15 and 30 min after injection. Insulin levels were measured by an enzyme-linked immunosorbent assay (ELISA) kit using a rat insulin standard (Morinaga, Yokohama, Japan) or the mouse insulin ELISA kit (ALPCO, Salem, NH, USA). Proinsulin was measured by the mouse proinsulin ELISA kit (ALPCO). All the experiments were carried out in male mice and were approved by the Animal Ethics Committee of Yamaguchi University School of Medicine.

Immunofluorescent staining of pancreatic islets

Pancreata were isolated from 12-week-old *Wfs1*$^{-/-}$ mice. Isolated pancreata were fixed overnight in 4% paraformaldehyde at room temperature. Tissue was then routinely processed for paraffin embedding, and 3-μm sections were cut and mounted on glass slides. The sections were immunostained with antibodies to insulin (Dako Cytomation, CA, USA), Glucagon (Santa Cruz, CA, USA), GRP78 (BD Biosciences, San Jose, CA, USA) and chromogranin A (Santa Cruz). The antibody raised against the 290 amino acid mouse WFS1-N-terminus has been described previously (9). Cy3- or fluorescein isothiocyanate-conjugated (FITC) secondary antibodies (Jackson Immunoresearch, West Grove, PA, USA) were used for fluorescence microscopy. Images were acquired on a confocal microscope (LSM 510, Carl Zeiss).

Evaluation of intragranular acidification

Islets were mechanically dissociated as previously described (15) to obtain dispersed islet cells. Cells were allowed to adhere on polylysine-coated plastic slides (Lab-Tek Chambered Coverglass, Nalge Nunc International, NY, USA) in RPMI medium, followed by 1 h pre-incubation with or without 100 nM bafilomycin A1 (Calbiochem) prior to DAMP and LysoTracker treatment. For DAMP staining, 3 μM DAMP (Invitrogen, OR, USA) was subsequently added to the medium for 1 h, and then dispersed islet cells were fixed with 4% paraformaldehyde in phosphate-buffered saline (PBS; pH 7.4). Anti-DNP-KLH secondary antibody (Molecular Probes, West Grove, PA, USA) was used for fluorescence microscopy. For LysoTracker (Molecular Probes) staining, 25 nM LysoTracker was added to the medium for 30 min. Then dispersed islet cells were fixed with 4% paraformaldehyde in PBS (pH 7.4). To recognize insulin-containing cells, after fixation, cells were stained with anti-insulin antibodies and visualized with FITC secondary antibodies. Fluorescent images were acquired with a confocal microscope, LSM 510 (Carl Zeiss). To measure fluorescence intensity derived from either DMAP or LysoTracker, a number of insulin-positive cells were randomly selected from both genotypes. The fluorescence intensity of each whole cell with the exception of the nucleus was measured and was later quantified using ImageJ 1.38× (36).

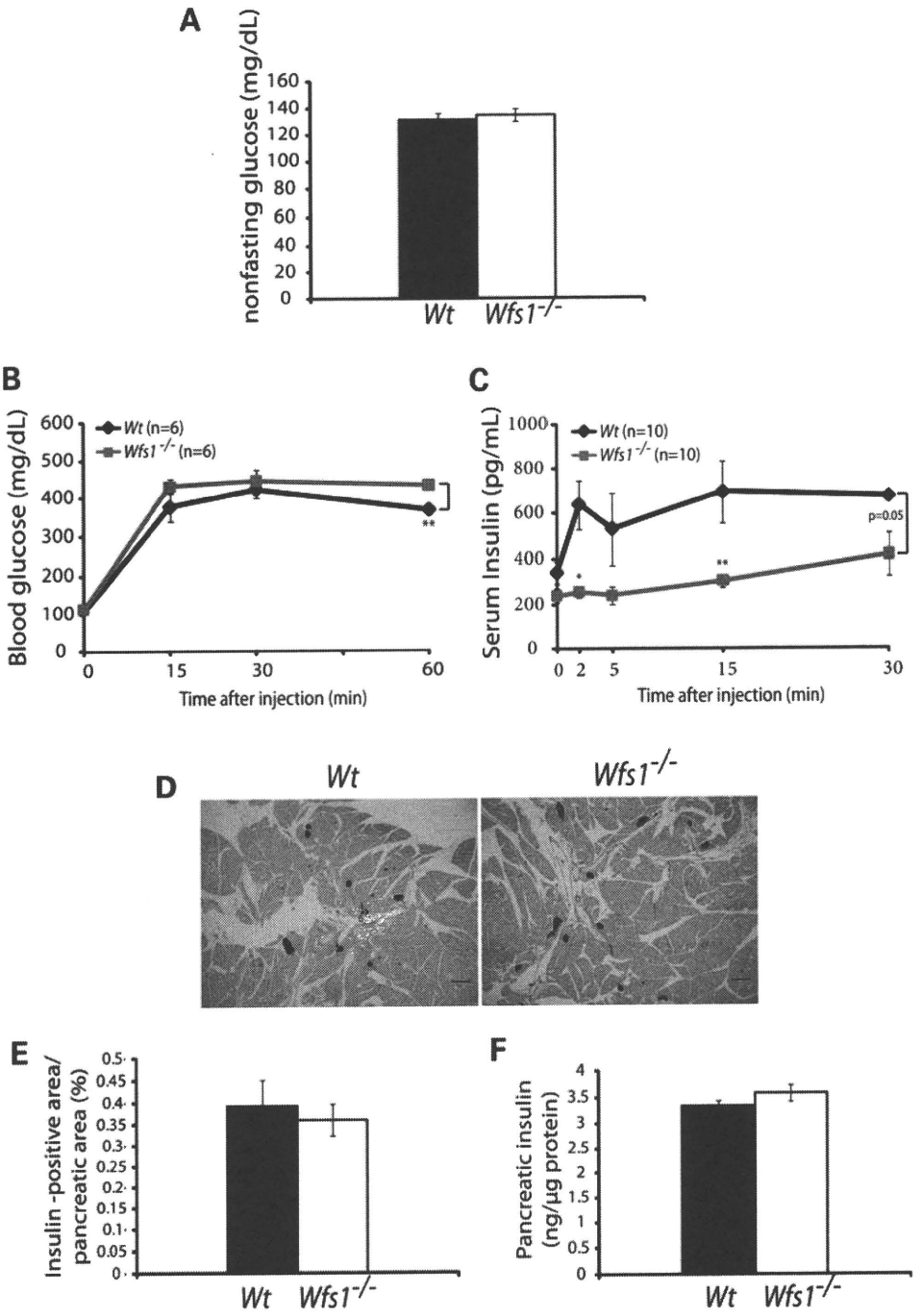

Figure 4. WFS1 deficiency results in glucose intolerance with severely impaired glucose-induced insulin release. (**A**) Non-fasting blood glucose levels in 12-week-old male mice (*Wt*, $n = 11$; *Wfs1*$^{-/-}$, $n = 11$). Intraperitoneal glucose tolerance tests were performed on overnight-fasted male *Wt* and *Wfs1*$^{-/-}$ mice at 12 weeks of age after intraperitoneal injection of D-glucose (2 g/kg) (**B** and **C**). (B) Glucose levels at the indicated time intervals. $^{*}P < 0.05$; $^{**}P < 0.01$ (*Wt*, $n = 6$; *Wfs1*$^{-/-}$, $n = 6$). (C) Plasma insulin levels at indicated time points after glucose injection (*Wt*, $n = 10$; *Wfs1*$^{-/-}$, $n = 10$). Random pancreatic sections from the entire pancreas of 12-week-old mice of the indicated genotypes were stained with antibodies to insulin and then counterstained with hematoxylin (**D** and **E**). (D) Representative photographs of indicated genotypes are shown. Scale bar represents 300 µm. (E) Insulin-immunoreactive area was measured. Results are expressed as % of total pancreatic area containing insulin-immunoreactive cells (*Wt*, $n = 3$; *Wfs1*$^{-/-}$, $n = 3$). (**F**) Insulin content extracted from whole pancreas of *Wt* and *Wfs1*$^{-/-}$ mice (*Wt*, $n = 15$; *Wfs1*$^{-/-}$, $n = 12$).

Measurement of β-cell area

All animals were anesthetized with sodium pentobarbital (65 mg/kg, intraperitoneally) and perfused intracardially with 4% paraformaldehyde. Isolated pancreatic tissues were then routinely processed for paraffin embedding, and 3 µm sections were cut and mounted on glass slides. The sections were de-paraffinized and re-hydrated, then immunostained with antibodies to insulin (Dako) bound to biotin-conjugated secondary antibodies with 3,3′-diaminobenzidine

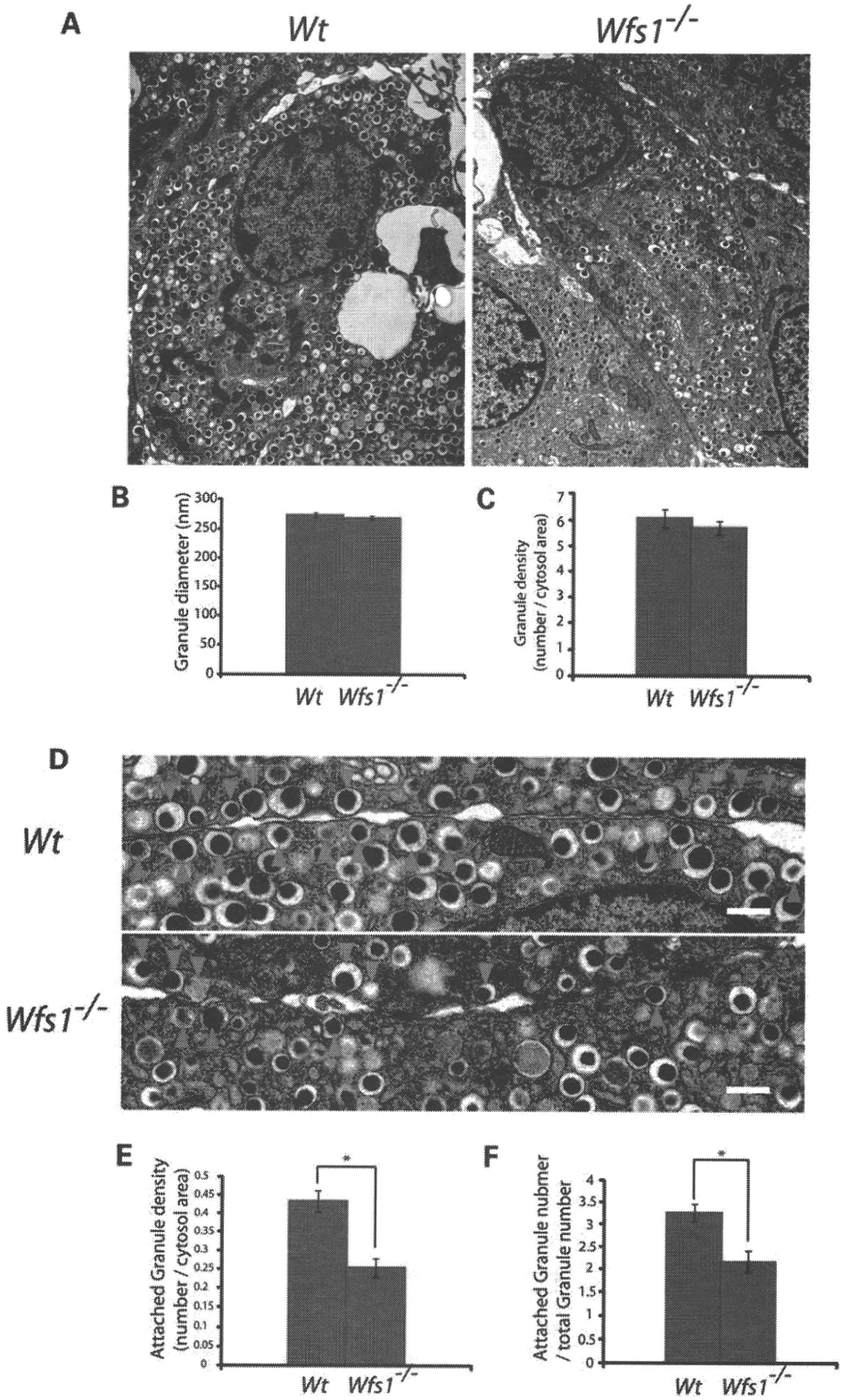

Figure 5. WFS1-deficient β-cells have reduced the number of dense-core secretory granules attached to the plasma membrane. Morphometric analyses of insulin granules in β-cells from *Wfs1*$^{-/-}$ and *Wt* mice. For each genotype, 20 randomly selected β-cells from two 12-week-old male mice were analyzed. (**A**) Electron micrographs of β-cell sections from *Wfs1*$^{-/-}$ and *Wt* mice. Scale bar represents 1 μm. (**B**) Average granule diameter and (**C**) granule number per cytosol area (μm^2). (**D**) Electron micrographs of insulin granules attached to the plasma membrane. Scale bars indicate 500 nm. (**E**) Average number of attached granules per cytosol area (μm^2) and (**F**) the attached granules to total granules ratio are summarized as the mean ± SEM in the graph. $^*P < 0.05$.

tetrahydrochloride and hematoxylin. The β-cell area was determined after analysis of a number of random sections from three mice in each genotype and analyzed with ImageJ 1.38×.

Isolation of islets from mice

Islets from 12-week-old C57BL/6J male mice, *Wfs1*$^{-/-}$ and *Wfs1*$^{+/-}$/C57BL/6J background male mice were isolated by ductal collagenase digestion of the pancreas (15) followed by filtering and washing through a 70-mm Nylon cell strainer (BD Biosciences). Isolated islets were then maintained in RPMI medium containing 11 mM glucose, 10% FBS, 200 U/ml of penicillin and 200 mg/ml of streptomycin in humidified 5% CO_2 and 95% air at 37°C. All experiments on isolated islets were carried out 15 h after isolation.

Preparation of total cell extract

Isolated islets were washed twice in ice-cold PBS and lysed in ice-cold cell lysis buffer consisting of 50 mM HEPES (pH 7.5), 1% (v/v) Triton X-100, 2 mM activated sodium orthovanadate, 100 mM sodium fluoride, 10 mM sodium pyrophosphate, 4 mM EDTA, 1 mM phenylmethylsulfonyl fluoride, 1 μg/ml of leupeptin and 1 μg/ml of aprotinin, then passed through a syringe with a 21 gauge needle 10 times, and particulate material was removed by centrifugation (10 000*g* for 10 min at 4°C). The supernatant was collected. Protein concentrations were determined using the BCA protein assay (Thermo Scientific, Rockford, IL, USA).

For immunoprecipitation, mouse insulinoma MIN6 cells were cultured in 100 mm diameter culture dishes until 80% confluence and lysed in ice-cold RIPA buffer consisting of 20 mM HEPES (pH 7.2), 100 mM NaCl, 25 mM NaF, 1 mM sodium vanadate, 1 mM benzamidine, 5 μg/ml of leupeptin, 5 μg/ml of aprotinin, 1 mM phenylmethylsulfonyl fluoride, 1 mM dithiothreitol and 0.5% NP-40 in the presence of 1 mM EDTA and centrifuged for 15 min at 15 000*g*. Immunoprecipitation was performed using anti-WFS1 antibody and protein A Sepharose. After washing, immune complexes were directly eluted from the Sepharose using RIPA buffer.

Western blot analysis

Proteins were resolved on 4–20 or 15–25% gradient polyacrylamide gels (Cosmo Bio Tokyo), blotted onto a PVDF membrane (Amersham Plc, Buckinghamshire, UK) and incubated overnight at 4°C in Tris-buffered saline containing a 1:500–1000 dilution of antibodies as listed below. The membrane was then incubated at 4°C for 60 min in Tris-buffered saline with a 1:5000 dilution of anti-rabbit IgG or anti-mouse IgG horseradish peroxidase–conjugated secondary antibody (Jackson Immunoresearch). Antibodies used were anti-WFS1 (9), anti-insulin/proinsulin (Dako), anti-PC2 (Gene Tex), anti-PC1/3 (Abcam, Cambridge, UK) and anti-mGAPDH (Sigma, St Louis, MO, USA). Immune complexes were revealed using an ECL Western Blot Detection kit (Amersham Plc) and the images were acquired by exposure onto medical X-ray film (Konica Minolta). Band intensities in the blots were later quantified using ImageJ 1.38× (36), and mGAPDH bands were used to adjust for loading differences.

Electron microscopy

Conventional electron microscopy was performed as described previously (14). In brief, isolated pancreases were routinely processed. Ultrathin sections were doubly stained with uranyl acetate and lead citrate, and then observed under an electron microscope (Tecnai^{TM} G^2 Spirit, FEI Company). The diameter and the density of secretory granules were analyzed and quantified using ImageJ 1.38× (36).

Immunoelectron microscopy

All animals were anesthetized with sodium pentobarbital (65 mg/kg, intraperitoneally) and perfused intracardially with ice-cold saline, followed by 0.5% glutaraldehyde and 4% paraformaldehyde in 0.1 M phosphate buffer (PB; pH 7.4). Pancreata were removed and soaked in 0.1 M PB containing 30% sucrose until they sank, and then frozen in powdered dry ice. Pancreatic sections were cut at a thickness of 60 μm using a cryostat. The free-floating sections were pre-incubated for 2 h with 20% normal goat serum (NGS) in PBS and bleached for 1 h with 50% methanol and 1.5% hydrogen peroxide at 4°C. After washing with PBS containing 0.05% NGS and 0.3% Triton X-100, the sections were incubated with anti-WFS1 diluted 1:200 in PBS containing 1% NGS for 2 days at 20°C. Then, the sections were incubated for 2 h at 20°C with biotinylated secondary antibody (Dako Cytomation, Glostrup, Denmark; diluted 1:500) in PBS containing 1% NGS, followed by incubation with a mixture of horseradish peroxidase and rabbit anti-horseradish peroxidase antibody complexes (PAP; Dako Cytomation) and peroxidase-conjugated streptavidin (Dako Cytomation, diluted 1:500) in PBS (PAP-BAP method) for 2 h at 20°C. Subsequently, they were washed in 0.05 M Tris–HCl buffer and colored by a nickel-enhanced DAB reaction. The sections were post-fixed for 1 h with 1% OsO_4 in 0.1 M PB, block-stained for 1 h with 2% uranyl acetate in distilled water, dehydrated with a graded series of ethanol rinses, infiltrated with propylene oxide and finally embedded in epoxy resin. Ultrathin sections were collected on copper grids and observed under a Tecnai^{TM} G^2 Spirit (FEI Company) electron microscope, operated at 120 kV with 2 min of lead staining. For immune-gold-electron microscopy, the pre-embedded immunogold method was used. Cryosections (60 μm) were incubated with anti-WFS1 diluted 1:100 in PBS containing 1% NGS for 5 days at 20°C, followed by incubation with secondary antibodies conjugated with colloidal gold (10 nm diameter, BB International, diluted 1:20). Quantification of the distribution of gold particles on secretory granules and ER was performed in representative sections of a number of cells ($n = 24$).

Statistical analysis

Data were obtained from at least three independent experiments and presented as mean ± SEM. The significance of variations was analyzed by one-factor Student's *t*-test with a significance level of 0.05 (95% confidence interval).

ACKNOWLEDGEMENTS

The authors would like to thank members of the division for helpful discussion.

Conflict of Interest statement. None declared.

FUNDING

This study was supported in part by Grants-in-Aid for Scientific Research (16390096, 18390103 and 20390093 to Y.T., 22590984 to K.T., 21500326 to K.S.) from the Ministry of Education, Culture, Sports, and Science, grants (to Y.O. and Y.T.) from the Ministry of Health, Labor and Welfare of Japan, grants from the Takeda Science Foundation (to Y.T. and K.T.) and a grant from Banyu Life Science Foundation (to K.T.).

REFERENCES

1. Wild, S., Roglic, G., Green, A., Sicree, R. and King, H. (2004) Global prevalence of diabetes: estimates for the year 2000 and projections for 2030. *Diabetes Care*, **27**, 1047–1053.
2. Donath, M.Y. and Halban, P.A. (2004) Decreased beta-cell mass in diabetes: significance, mechanisms and therapeutic implications. *Diabetologia*, **47**, 581–589.
3. Rhodes, C.J. (2005) Type 2 diabetes-a matter of beta-cell life and death? *Science*, **307**, 380–384.
4. Porter, J.R. and Barrett, T.G. (2005) Monogenic syndromes of abnormal glucose homeostasis: clinical review and relevance to the understanding of the pathology of insulin resistance and beta cell failure. *J. Med. Genet.*, **42**, 893–902.
5. Barrett, T.G. and Bundey, S.E. (1997) Wolfram (DIDMOAD) syndrome. *J. Med. Genet.*, **34**, 838–841.
6. Karasik, A., O'Hara, C., Srikanta, S., Swift, M., Soeldner, J.S., Kahn, C.R. and Herskowitz, R.D. (1989) Genetically programmed selective islet beta-cell loss in diabetic subjects with Wolfram's syndrome. *Diabetes Care*, **12**, 135–138.
7. Inoue, H., Tanizawa, Y., Wasson, J., Behn, P., Kalidas, K., Bernal-Mizrachi, E., Mueckler, M., Marshall, H., Donis-Keller, H., Crock, P. *et al.* (1998) A gene encoding a transmembrane protein is mutated in patients with diabetes mellitus and optic atrophy (Wolfram syndrome). *Nat. Genet.*, **20**, 143–148.
8. Strom, T.M., Hortnagel, K., Hofmann, S., Gekeler, F., Scharfe, C., Rabl, W., Gerbitz, K.D. and Meitinger, T. (1998) Diabetes insipidus, diabetes mellitus, optic atrophy and deafness (DIDMOAD) caused by mutations in a novel gene (Wolframin) coding for a predicted transmembrane protein. *Hum. Mol. Genet.*, **7**, 2021–2028.
9. Takeda, K., Inoue, H., Tanizawa, Y., Matsuzaki, Y., Oba, J., Watanabe, Y., Shinoda, K. and Oka, Y. (2001) WFS1 (Wolfram syndrome 1) gene product: predominant subcellular localization to endoplasmic reticulum in cultured cells and neuronal expression in rat brain. *Hum. Mol. Genet.*, **10**, 477–484.
10. Takei, D., Ishihara, H., Yamaguchi, S., Yamada, T., Tamura, A., Katagiri, H., Maruyama, Y. and Oka, Y. (2006) WFS1 protein modulates the free Ca(2+) concentration in the endoplasmic reticulum. *FEBS Lett.*, **580**, 5635–5640.
11. Riggs, A.C., Bernal-Mizrachi, E., Ohsugi, M., Wasson, J., Fatrai, S., Welling, C., Murray, J., Schmidt, R.E., Herrera, P.L. and Permutt, M.A. (2005) Mice conditionally lacking the Wolfram gene in pancreatic islet beta cells exhibit diabetes as a result of enhanced endoplasmic reticulum stress and apoptosis. *Diabetologia*, **48**, 2313–2321.
12. Yamada, T., Ishihara, H., Tamura, A., Takahashi, R., Yamaguchi, S., Takei, D., Tokita, A., Satake, C., Tashiro, F., Katagiri, H. *et al.* (2006) WFS1-deficiency increases endoplasmic reticulum stress, impairs cell cycle progression and triggers the apoptotic pathway specifically in pancreatic beta-cells. *Hum. Mol. Genet.*, **15**, 1600–1609.
13. Fonseca, S.G., Fukuma, M., Lipson, K.L., Nguyen, L.X., Allen, J.R., Oka, Y. and Urano, F. (2005) WFS1 is a novel component of the unfolded protein response and maintains homeostasis of the endoplasmic reticulum in pancreatic beta-cells. *J. Biol. Chem.*, **280**, 39609–39615.
14. Akiyama, M., Hatanaka, M., Ohta, Y., Ueda, K., Yanai, A., Uehara, Y., Tanabe, K., Tsuru, M., Miyazaki, M., Saeki, S. *et al.* (2009) Increased insulin demand promotes while pioglitazone prevents pancreatic beta cell apoptosis in WFS1 knockout mice. *Diabetologia*, **52**, 653–663.
15. Ishihara, H., Takeda, S., Tamura, A., Takahashi, R., Yamaguchi, S., Takei, D., Yamada, T., Inoue, H., Soga, H., Katagiri, H. *et al.* (2004) Disruption of the WFS1 gene in mice causes progressive beta-cell loss and impaired stimulus-secretion coupling in insulin secretion. *Hum. Mol. Genet.*, **13**, 1159–1170.
16. Osman, A.A., Saito, M., Makepeace, C., Permutt, M.A., Schlesinger, P. and Mueckler, M. (2003) Wolframin expression induces novel ion channel activity in endoplasmic reticulum membranes and increases intracellular calcium. *J. Biol. Chem.*, **278**, 52755–52762.
17. Schoonderwoert, V.T. and Martens, G.J. (2001) Proton pumping in the secretory pathway. *J. Membr. Biol.*, **182**, 159–169.
18. Barg, S., Huang, P., Eliasson, L., Nelson, D.J., Obermuller, S., Rorsman, P., Thevenod, F. and Renstrom, E. (2001) Priming of insulin granules for exocytosis by granular Cl(-) uptake and acidification. *J. Cell. Sci.*, **114**, 2145–2154.
19. Ueda, K., Kawano, J., Takeda, K., Yujiri, T., Tanabe, K., Anno, T., Akiyama, M., Nozaki, J., Yoshinaga, T., Koizumi, A. *et al.* (2005) Endoplasmic reticulum stress induces WFS1 gene expression in pancreatic beta-cells via transcriptional activation. *Eur. J. Endocrinol.*, **153**, 167–176.
20. Hofmann, S., Philbrook, C., Gerbitz, K.D. and Bauer, M.F. (2003) Wolfram syndrome: structural and functional analyses of mutant and wild-type Wolframin, the WFS1 gene product. *Hum. Mol. Genet.*, **12**, 2003–2012.
21. Anderson, R.G., Falck, J.R., Goldstein, J.L. and Brown, M.S. (1984) Visualization of acidic organelles in intact cells by electron microscopy. *Proc. Natl Acad. Sci. USA*, **81**, 4838–4842.
22. Louagie, E., Taylor, N.A., Flamez, D., Roebroek, A.J., Bright, N.A., Meulemans, S., Quintens, R., Herrera, P.L., Schuit, F., Van de Ven, W.J. *et al.* (2008) Role of furin in granular acidification in the endocrine pancreas: identification of the V-ATPase subunit Ac45 as a candidate substrate. *Proc. Natl Acad. Sci. USA*, **105**, 12319–12324.
23. Davidson, H.W., Rhodes, C.J. and Hutton, J.C. (1988) Intraorganellar calcium and pH control proinsulin cleavage in the pancreatic beta cell via two distinct site-specific endopeptidases. *Nature*, **333**, 93–96.
24. Smeekens, S.P., Montag, A.G., Thomas, G., Albiges-Rizo, C., Carroll, R., Benig, M., Phillips, L.A., Martin, S., Ohagi, S., Gardner, P. *et al.* (1992) Proinsulin processing by the subtilisin-related proprotein convertases furin, PC2, and PC3. *Proc. Natl Acad. Sci. USA*, **89**, 8822–8826.
25. Zhu, X., Orci, L., Carroll, R., Norrbom, C., Ravazzola, M. and Steiner, D.F. (2002) Severe block in processing of proinsulin to insulin accompanied by elevation of des-64,65 proinsulin intermediates in islets of mice lacking prohormone convertase 1/3. *Proc. Natl Acad. Sci. USA*, **99**, 10299–10304.
26. Orci, L., Halban, P., Perrelet, A., Amherdt, M., Ravazzola, M. and Anderson, R.G. (1994) pH-independent and -dependent cleavage of proinsulin in the same secretory vesicle. *J. Cell. Biol.*, **126**, 1149–1156.
27. Guest, P.C., Abdel-Halim, S.M., Gross, D.J., Clark, A., Poitout, V., Amaria, R., Ostenson, C.G. and Hutton, J.C. (2002) Proinsulin processing in the diabetic Goto-Kakizaki rat. *J. Endocrinol.*, **175**, 637–647.
28. Renstrom, E., Eliasson, L., Bokvist, K. and Rorsman, P. (1996) Cooling inhibits exocytosis in single mouse pancreatic B-cells by suppression of granule mobilization. *J. Physiol.*, **494** (Pt 1), 41–52.
29. Renstrom, E., Eliasson, L. and Rorsman, P. (1997) Protein kinase A-dependent and -independent stimulation of exocytosis by cAMP in mouse pancreatic B-cells. *J .Physiol.*, **502** (Pt 1), 105–118.
30. Eliasson, L., Renstrom, E., Ding, W.G., Proks, P. and Rorsman, P. (1997) Rapid ATP-dependent priming of secretory granules precedes Ca(2+)-induced exocytosis in mouse pancreatic B-cells. *J. Physiol.*, **503** (Pt 2), 399–412.
31. Deriy, L.V., Gomez, E.A., Jacobson, D.A., Wang, X., Hopson, J.A., Liu, X.Y., Zhang, G., Bindokas, V.P., Philipson, L.H. and Nelson, D.J. (2009) The granular chloride channel ClC-3 is permissive for insulin secretion. *Cell Metab.*, **10**, 316–323.
32. Li, D.Q., Jing, X., Salehi, A., Collins, S.C., Hoppa, M.B., Rosengren, A.H., Zhang, E., Lundquist, I., Olofsson, C.S., Morgelin, M. *et al.* (2009) Suppression of sulfonylurea- and glucose-induced insulin secretion in

vitro and in vivo in mice lacking the chloride transport protein ClC-3. *Cell Metab.*, **10**, 309–315.
33. Zatyka, M., Ricketts, C., da Silva Xavier, G., Minton, J., Fenton, S., Hofmann-Thiel, S., Rutter, G.A. and Barrett, T.G. (2008) Sodium-potassium ATPase 1 subunit is a molecular partner of Wolframin, an endoplasmic reticulum protein involved in ER stress. *Hum. Mol. Genet.*, **17**, 190–200.
34. Yurimoto, S., Hatano, N., Tsuchiya, M., Kato, K., Fujimoto, T., Masaki, T., Kobayashi, R. and Tokumitsu, H. (2009) Identification and characterization of Wolframin, the product of the wolfram syndrome gene (WFS1), as a novel calmodulin-binding protein. *Biochemistry*, **48**, 3946–3955.
35. Fonseca, S.G., Ishigaki, S., Oslowski, C.M., Lu, S., Lipson, K.L., Ghosh, R., Hayashi, E., Ishihara, H., Oka, Y., Permutt, M.A. *et al.* (2000) Wolfram syndrome 1 gene negatively regulates ER stress signaling in rodent and human cells. *J. Clin. Invest.*, **120**, 744–755.
36. Girish, V. and Vijayalakshmi, A. (2004) Affordable image analysis using NIH Image/ImageJ. *Indian J. Cancer*, **41**, 47.

Glucose and Fatty Acids Synergize to Promote B-Cell Apoptosis through Activation of Glycogen Synthase Kinase 3β Independent of JNK Activation

Katsuya Tanabe[1], Yang Liu[1], Syed D. Hasan[1], Sara C. Martinez[1], Corentin Cras-Méneur[1], Cris M. Welling[1], Ernesto Bernal-Mizrachi[1], Yukio Tanizawa[3], Christopher J. Rhodes[4], Erik Zmuda[5], Tsonwin Hai[5], Nada A. Abumrad[2], M. Alan Permutt[1]*

1 Division of Endocrinology, Metabolism, and Lipid Research, Washington University School of Medicine, St. Louis, Missouri, United States of America, **2** Division of Nutritional Science, Department of Medicine, Washington University School of Medicine, St. Louis, Missouri, United States of America, **3** Division of Endocrinology, Metabolism, Hematological Sciences and Therapeutics Department of Bio-Signal Analysis, Yamaguchi University Graduate School of Medicine, Ube, Yamaguchi, Japan, **4** Department of Medicine, Kovler Diabetes Center, University of Chicago, Chicago, Illinois, United States of America, **5** Department of Molecular and Cellular Biochemistry, Center for Molecular Neurobiology, Ohio State University, Columbus, Ohio, United States of America

Abstract

Background: The combination of elevated glucose and free-fatty acids (FFA), prevalent in diabetes, has been suggested to be a major contributor to pancreatic β-cell death. This study examines the synergistic effects of glucose and FFA on β-cell apoptosis and the molecular mechanisms involved. Mouse insulinoma cells and primary islets were treated with palmitate at increasing glucose and effects on apoptosis, endoplasmic reticulum (ER) stress and insulin receptor substrate (IRS) signaling were examined.

Principal Findings: Increasing glucose (5–25 mM) with palmitate (400 μM) had synergistic effects on apoptosis. Jun NH2-terminal kinase (JNK) activation peaked at the lowest glucose concentration, in contrast to a progressive reduction in IRS2 protein and impairment of insulin receptor substrate signaling. A synergistic effect was observed on activation of ER stress markers, along with recruitment of SREBP1 to the nucleus. These findings were confirmed in primary islets. The above effects associated with an increase in glycogen synthase kinase 3β (Gsk3β) activity and were reversed along with apoptosis by an adenovirus expressing a kinase dead Gsk3β.

Conclusions/Significance: Glucose in the presence of FFA results in synergistic effects on ER stress, impaired insulin receptor substrate signaling and Gsk3β activation. The data support the importance of controlling both hyperglycemia and hyperlipidemia in the management of Type 2 diabetes, and identify pancreatic islet β-cell Gsk3β as a potential therapeutic target.

Citation: Tanabe K, Liu Y, Hasan SD, Martinez SC, Cras-Méneur C, et al. (2011) Glucose and Fatty Acids Synergize to Promote B-Cell Apoptosis through Activation of Glycogen Synthase Kinase 3β Independent of JNK Activation. PLoS ONE 6(4): e18146. doi:10.1371/journal.pone.0018146

Editor: Kathrin Maedler, University of Bremen, Germany

Received July 6, 2010; **Accepted** February 27, 2011; **Published** April 26, 2011

Funding: This work was supported by National Institutes of Health (NIH) grants R37 DK16746 to M.A. Permutt, R01 DK33301 to N.A. Abumrad, RO1 DK64938 to T. Hai, NIH P60 DK20579 to the Washington University DRTC, and NIH P30DK056341 to the Adipocyte Biology and Molecular Nutrition Core of the Nutrition Obesity Research Center. Katsuya Tanabe was granted from Grants-in-Aid for Scientific Research (22590984) from Ministry of Education, Culture, Sports and Science, a grant from Takeda Science Foundation and a grant from Banyu Life Science Foundation Japan. The funders had no role in study design, data collection and analysis, decision to publish, or preparation of the manuscript.

Competing Interests: The authors have declared that no competing interests exist.

* E-mail: apermutt@dom.wustl.edu

Introduction

The natural history of Type 2 diabetes mellitus (T2D) includes a progressive decline in β-cell function associated with peripheral insulin resistance. The β-cell dysfunction has been attributed in part to loss of β-cell mass via apoptosis [1] with inadequate insulin secretion leading to hyperglycemia and other diabetes symptoms [2]. Insulin resistance is at the core of obesity associated diabetes and is thought to reflect impaired insulin signaling due to chronically increased levels of free fatty acids (FFA). High FFA are also implicated in the reduction in β-cell mass that has been referred to as lipotoxicity. The combination of elevated glucose and FFA, or "glucolipotoxicity" that is prevalent in T2D has been suggested to be a major contributor to β-cell death [3,4,5,6].

The search for molecular mechanisms for glucose potentiation of FFA- induced β-cell dysfunction has been the subject of several recent studies (see [7] for review). One area of investigation has focused on the insulin receptor substrate-PI3K-Akt signaling pathway. The first study showing that the FFA oleate impaired insulin signaling in insulinoma cells demonstrated that the cells were protected from FFA-induced apoptosis by expressing a constitutively active Akt [8]. Several biochemical and genetic studies subsequently showed that saturated FFA could promote ER stress in insulinoma cells and in primary rodent and human islets [9,10,11,12]. More recently, it was shown that high glucose

potentiated FFA induced apoptosis by enhancing ER stress [13]. ER stress in insulinoma cells was shown to impair insulin signaling through activation of ATF3, an ER stress response protein that was implicated in suppression of IRS2 expression [14]. ATF3 is another stress inducible gene that is activated in different tissues by a variety of stresses [15].

How glucose potentiates FFA induced ER stress, reduced insulin receptor substrate signaling, and apoptosis is incompletely understood. Our recent study showed that there was a dose-dependent effect of FFA in the presence of high glucose on apoptosis in insulinoma cells and primary islets [16] that was associated with JNK activation, ER stress, and reduced insulin signaling. In the current study, we found a dose-dependent effect of glucose in the presence of palmitate on cell death that appeared to be over and above JNK activation. We observed glucose dose-dependent synergistic effects on palmitate inhibition of receptor substrate signaling and activation of Gsk3β. Co-treatment with an adenovirus expressing a kinase dead Gsk3β significantly protected β-cells from cell death. Our data support importance of Gsk3β in the synergistic effects of glucose and FFA.

Materials and Methods

Cell Culture

Mouse insulinoma cell line MIN6 (passage 24–32) were grown in monolayer cultures as described previously [17] in Dulbecco's modified Eagle's medium (Sigma Aldrich) supplemented with 15% fetal bovine serum, 50 mmol/L β-mercaptoethanol at 37°C in a humidified (5% CO_2, 95% air) atmosphere. Rat insulinoma INS-r3 cells were grown as previously described [18]. The palmitic acid (palmitate), formalin, propidium iodide, IL-1b, tunicamycin and TNFα were purchased from Sigma (Saint Louis, MO). Tauroursodeoxycholic Acid Sodium Salt (TUDCA) was purchased from CALBIOCEM (Darmstadt, Germany).

Fatty acids (FFA) Treatment of MIN6 Cells and Islets

The complete protocol was previously described [16]. Briefly a 20 mM solution of the FFA in 0.01 M NaOH was incubated at 70°C for 30 minutes. Then, 330 µL of 30% BSA and 400 µL of the free FFA/NaOH mixture was mixed together and filter sterilized with 20 mL of either the DMEM or RPMI media. The approximate molar ratio of FFA:BSA is 6:1 with 400 µM palmitate. The addition of BSA or a FFA:BSA mixture has not been shown to affect the pH of the media.

Propidium iodide/Cell Death Assay

MIN6 cells were grown on glass cover slips within the wells of a 6-well plate and incubated with either BSA alone or 400 µM both FFAs complexed with BSA for 24 hours as previously described [16]. After treating cells for 24 hours with various treatments, the cells were incubated with 10 µg/ml (1 to 1000 dilution) Propidium Iodide (PI) and 20 ug DAPI added directly to the media at 37°C, 5% CO2 for 1 hour. The medium was then removed by aspiration, and the cells were washed once with PBS and then fixed by incubation with 3.7% formaldehyde for 15 min at room temperature. After fixation, the MIN6 cells were mounted with anti-fading gel solution including DAPI (Biomeda Corporation, Foster City, CA) on to glass slides. Each condition reported represents over 3000 cells counted by randomized field selection. The percentage of cell-death is reported as the number of PI stained nuclei over the total number of nuclei stained by DAPI as quantitated by Image J software 1.37 [19].

Western blot analysis

MIN6 were washed twice in ice-cold phosphate-buffered saline and were lysed in ice-cold cell lysis buffer consisting of 50 mM HEPES (pH 7.5), 1% (v/v) Nonidet P-40, 2 mM activated sodium orthovanadate, 100 mM sodium fluoride, 10 mM sodium pyrophosphate, 4 mM EDTA, 1 mM phenylmethylsulfonyl fluoride, 1 µg/mL leupeptin, and 1 µg/mL aprotinin, then passed through syringe with a 21 gauge needle 10 times while INS-r3 cells were sonicated (Misonix, Farmingdale, NY) and particulate material from both cell lines were removed by centrifugation (10,000× g; 10 min; 4°C). The supernatants were collected. Protein concentrations were determined using the Bio-Rad protein assay (Bio-Rad, Hercules, CA).

The extracts (20 µg of total protein) were resolved on 7.5% or 4–15% gradient polyacrylamide gels and were blotted onto a nitrocellulose membrane (Bio-Rad, CA), and incubated overnight at 4°C in Tris-buffered saline containing a 1:1000–5000 dilution of antibody as listed below. The membrane was then incubated at 4°C for 60 min in Tris-buffered saline with a 1:2000 dilution of anti-rabbit IgG or anti-mouse IgG horseradish peroxidase-conjugated secondary antibody (Cell Signaling Technology). Antibodies used were anti-total Akt, anti-phospho-Akt (S473), anti-cleaved Caspase3, anti-phospho-PERK (980Thr), anti-phospho-eIF2α(51Ser), anti-total JNK1/2, anti-phospho-JNK, anti-phospho-AMPK, total AMPK, anti-phospho-ACC, anti-total ACC from Cell Signaling Technology (Beverley, MA), anti-SREBP1 from Neo Markers (Fremont, CA), anti-IRS1, anti-IRS2 from Upstate (Billerica, MA), anti-ATF3, anti-Insig1, anti-Lamin from Santa Cruz (Santa Cruz, CA) and anti-α-Tubulin and from Sigma (Saint Louis, MO).

Immune complexes were revealed using ECL Advance Western Blot Detection kit (Amersham Plc, Buckinghamshire UK) and the images were acquired using a FluoroChem 8800 digital camera acquisition system (Alpha Innotech, San Leandro, CA, USA). Band intensities in the blots were later quantified using ImageJ 1.38× [19] and α-Tubulin or β-Actin bands were used to adjust for loading differences.

Nuclear and cytoplasmic fractions from MIN6

MIN6 cells were cultured in 60-mm diameter culture dishes until 80% confluency. For isolation of nuclear extracts, the cells were then collected into microtubes, centrifuged for 20 s in a microcentrifuge, and resuspended in 200 µl of 10.0 mM Hepes, pH 7.9, containing 10.0 mM KCl, 1.5 mM $MgCl_2$, and 0.5 mM dithiothreitol. After incubation at 4°C for 15 min, the cells were lysed by passing 10 times through a 21-gauge needle. Next, the cells were centrifuged for 20s in a microcentrifuge, and the supernatant (cytoplasmic fraction) was removed and frozen in small aliquots. The pellet, which contained the nuclei, was resuspended in 150 µl of 20 mM Hepes, pH 7.9, containing 20% v/v glycerol, 0.1 M KCl, 0.2 mM EDTA, 0.5 mM dithiothreitol, and 0.5 mM phenylmethanesulfonyl fluoride and then stirred at 4°C for 30 min. The nuclear extracts were then centrifuged for 20 min at 4°C in a microcentrifuge. The supernatant was collected, aliquoted into small volumes, and stored at −80°C.

Islet isolation and culture

Islets from 12 weeks of age C57BL/6 male mice were isolated by ductal collagenase distension/digestion of the pancreas [20] followed by filtering and washing through a 70 mm Nylon cell strainer (BD Biosciences, San Jose, CA). Isolated islets were then maintained in RPMI medium containing 11 mM glucose, 10% FBS, 200 units/ml penicillin, and 200/ml streptomycin in humidified 5% CO2, 95% air at 37C. The palmitate treatments were carried out 15 hours after isolation. Adenovirus infections

A.

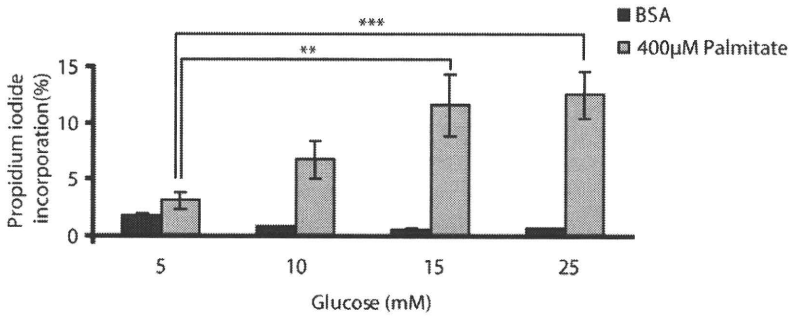
BSA
400μM Palmitate
***
**
Propidium iodide incorporation(%)
15
10
5
0
5
10
15
25
Glucose (mM)

B.

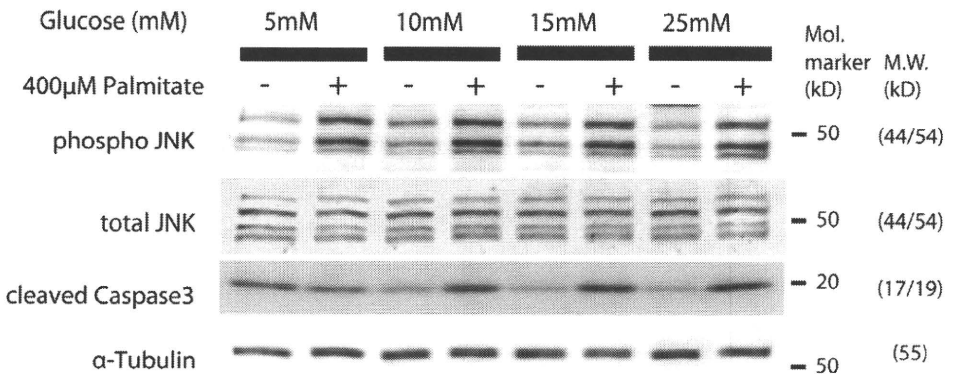
Glucose (mM)
5mM
10mM
15mM
25mM
400μM Palmitate
- + - + - + - +
Mol. marker (kD)
M.W. (kD)
phospho JNK
50
(44/54)
total JNK
50
(44/54)
cleaved Caspase3
20
(17/19)
α-Tubulin
50
(55)

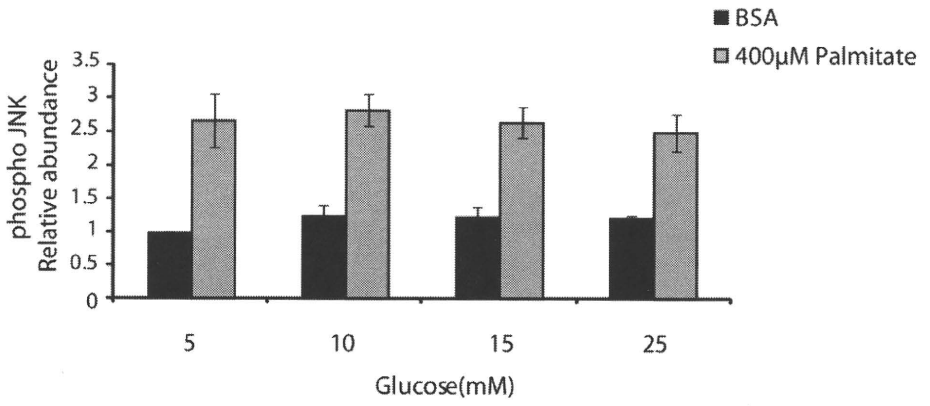
BSA
400μM Palmitate
phospho JNK Relative abundance
3.5
3
2.5
2
1.5
1
0.5
0
5
10
15
25
Glucose(mM)

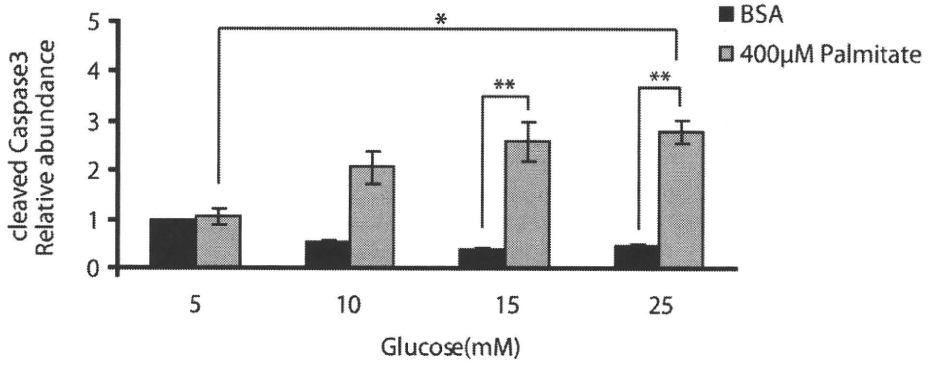
BSA
400μM Palmitate
*
**
**
cleaved Caspase3 Relative abundance
5
4
3
2
1
0
5
10
15
25
Glucose(mM)

Figure 1. Synergistic effects of glucose and palmitate on cell death but not JNK activation in MIN6 cells. MIN6 cells were treated with either control 0.5% BSA or 400 μM palmitate+0.5% BSA at a concentration of 5, 10, 15, 25 mM glucose for 24-h. (**A**) The percentage of cell death was then assessed by adding propidium iodide for the last hour of incubation as described under Methods. The bar graph depicts the averages of the data obtained from five individual experiments, and data are expressed as means ±S.E.M. ** $p<0.01$, *** $p<0.001$; (**B**) The cell lysates were subjected to Western blot analysis using anti-cleaved Caspase3, anti-phospho-JNK, anti-total JNK and anti-α-Tubulin antibodies. Protein level of phospho-JNK was normalized over total JNK. Cleaved Caspase3 levels were normalized over α-Tubulin. The representative result of three individual experiments is shown. The data obtained from three individual experiments are expressed as means ± S.E.M. * $p<0.05$, ** $p<0.01$.
doi:10.1371/journal.pone.0018146.g001

were initiated immediately following isolation at 500 multiplicity of infection (MOI). Infections were incubated for 15 hours and residual virus was removed prior to palmitate treatment. All procedures were performed in accordance with Washington University's Animal Studies Committee. The Principles of laboratory animal care (NIH publication no. 85–23, revised 1985; http://grants1.nih.gov/grants/olaw/references/phspol.htm) were followed.

Loss-of-function of ATF3 with shATF3

INS-r3 cells were seeded 24 hours prior to infection to achieve 70 percent confluence at time of infection. Control and ATF3

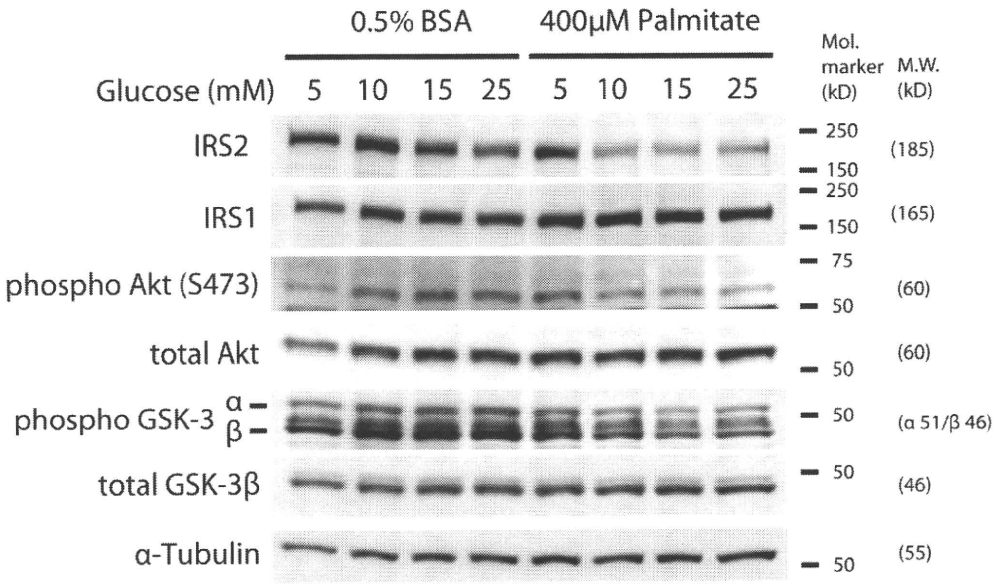

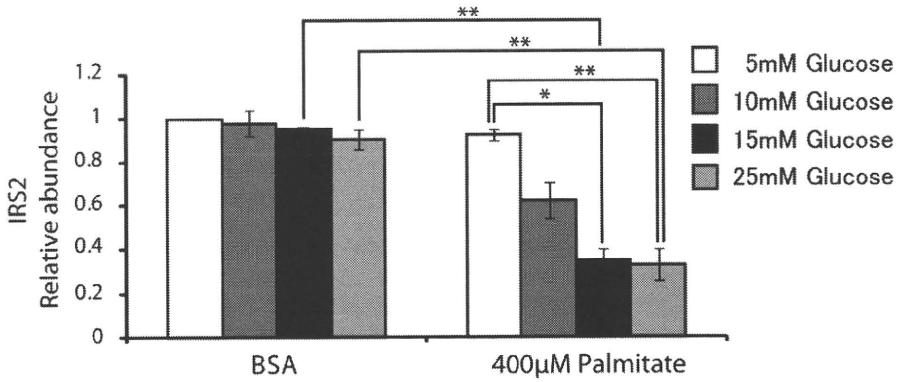

Figure 2. Glucose and palmitate potentiate to reduce insulin signaling. MIN6 cells were treated with either control 0.5% BSA (four lanes on left) or 400 μM palmitate+0.5% BSA (four lanes on right) at a concentration of 5, 10, 15, 25 mM glucose for 24-h. Total cell lysates were obtained and were subjected to Western blot analysis with antibodies to the indicated proteins. Protein level of IRS2 was normalized over α-Tubulin. The representative results of three individual experiments are shown. The results for IRS2 are graphically illustrated, data are expressed as means ±S.E.M. *$p<0.05$, **$p<0.01$.
doi:10.1371/journal.pone.0018146.g002